

Quantum phases of a frustrated spin-1 system: the 5/7 skewed ladder

Sambunath Das,^{1,*} Dayasindhu Dey,^{1,†} Manoranjan Kumar,^{2,‡} and S. Ramasesha^{1,§}

¹*Solid State and Structural Chemistry Unit, Indian Institute of Science, Bangalore 560012, India*

²*S. N. Bose National Centre for Basic Sciences,*

Block - JD, Sector - III, Salt Lake, Kolkata - 700106, India

(Dated: June 30, 2022)

The quantum phases in a spin-1 skewed ladder system formed by alternately fusing five- and seven-membered rings is studied numerically using exact diagonalization technique up to 16 spins and using density matrix renormalization group method for larger system sizes. The ladder has isotropic antiferromagnetic (AF) exchange interaction ($J_2 = 1$) between the nearest neighbor spins along the legs, varying isotropic AF exchange interaction (J_1) along the rungs. As a function of J_1 , the system shows many interesting ground states (gs) which vary from different types of nonmagnetic gs to different types of ferrimagnetic gs. Study of different gs properties such as spin gap, spin-spin correlations, spin density and bond order reveal that the system has four distinct phases namely, AF phase at small J_1 , ferrimagnetic phase with gs spin $S_G = 1$ per unit cell for $1.5 < J_1 < 4.7$ and with $S_G = 2$ for $J_1 > 5.9$, a reentrant AF phase at $4.8 < J_1 < 5.9$. The system also shows the presence of spin current at specific J_1 values due to simultaneously breaking of both reflection symmetry and spin parity symmetry.

I. INTRODUCTION

In low dimensional magnetic systems, confinement leads to strong quantum fluctuations, and these systems can show many exotic phases in the presence of frustration induced by the topology of exchange interactions^{1–21}. Even in a one dimensional (1D) spin system, with only nearest neighbor Heisenberg antiferromagnetic (HAF) exchange interaction, the ground state (gs) can be gapped or gapless for integer or half odd-integer spins, respectively, as pointed out in a seminal paper by Haldane²². The gs of the HAF integer spin chain can be represented as a valance bond solid (VBS)^{23–25}, and in 1987 Affleck, Kennedy, Lieb, and Tasaki (AKLT) showed that perfect VBS state may exist on various geometries with specific spins^{23,24}. The AKLT state still continues to inspire physicist for various reasons, for example, the AKLT state has led to many recent developments such as matrix product states technique^{26–28} which is a form of Density matrix renormalization group (DMRG) method^{29–32}, Tensor Network method³³ and projected entangled pair states ansatz^{27,28}. AKLT states can also be represented as cluster states which can be used in measurement-based quantum computation^{34,35}, and recently these states are explored in spin-3/2 on a hexagonal lattice^{36,37}.

The HAF spin-1 chain exhibits a topological phase, spin-1/2 edge modes, and the gs is four fold degenerate in the thermodynamic limit. The correlation length in the gs of spin-1 is 6.05 lattice units and the eigenvalue spectrum has large spin gaps^{38,39}. The gs can be represented as a VBS, which belongs to the same universality class of AKLT states^{23,24}. The two leg HAF spin-1 ladder shows interesting properties like plaquette-singlet solid state (PSSS) where two spin-1/2 singlet dimer are sitting at each rung and there is no overlap between the VBS states in the large rung exchange limit⁴⁰. The AKLT state in the system breaks down for any finite

value of rung exchange interaction⁴⁰. The spin-1 zigzag ladder shows a transition from Haldane phase to double Haldane phase^{41,42}. In fact the zigzag ladder can be mapped into a chain system with nearest neighbor and next nearest neighbor exchange interactions, and the gs of the frustrated systems is a singlet. In this work we explore the magnetic phases and phases of a spin-1 system on a 5/7-skewed ladder system; it has been demonstrated that a spin-1/2 system on this lattice shows many exotic phases⁴³.

The 5/7-skewed ladder is inspired by fused Azulene, a ladder like structure made up of 5- and 7-membered carbon rings alternately fused on a chain, studied by Thomas et al. in which they showed that the gs is ferrimagnetic⁴⁴. These structures can be mapped to zigzag like ladder structure with some missing bonds^{43,44}. The HAF spin-1/2 system on various lattices such as the 5/7, 3/4, 3/5, 5/5 are studied and it was shown that gs of these systems exhibit many interesting magnetic and non-magnetic ground states in their quantum phase diagrams with strength of the rung exchange interaction as a phase parameter⁴³. In the large rung exchange limit the gs wavefunction of 5/7 skewed ladder can be represented as product of rung singlet dimers and two ferromagnetically interacting spins per unit cell⁴⁵. In various parameter regimes this system shows dimer, spiral and chiral vector phases⁴³. In the presence of an axial magnetic field the HAF spin-1/2 system on the 5/7 skewed ladder exhibits four magnetization plateau phases⁴⁵.

The structure of zigzag, and 5/7 skewed ladder are shown in Figs. 1(a) and (b), and by periodically removing some of rung bonds, shown in red, from Fig. 1(a) to give 5/7 skewed ladder in Fig. 1(b). In this paper we are interested in the gs phases of spin-1 5/7 skewed ladder as a function of the ratio of rung to leg exchanges J_1 and J_2 respectively. We show that this system is highly frustrated, and in the small rung interaction limit, $J_1/J_2 < 1.0$, singlet dimers along the rung are

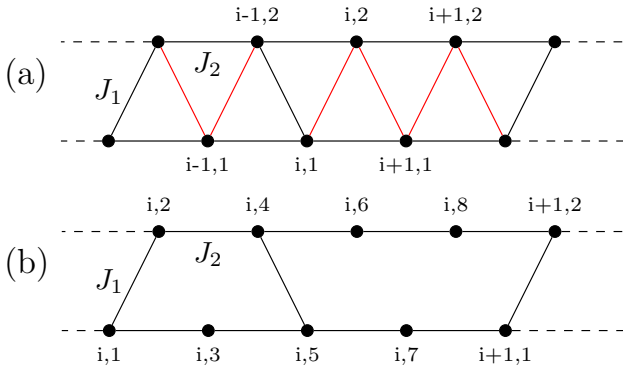


FIG. 1. Schematic diagram of (a) zigzag ladder. The nearest neighbor or rung interaction is J_1 and the next nearest neighbor (along the leg) interaction is J_2 . (b) 5/7 skewed ladder: some rung bonds shown in red of the zigzag ladder are periodically removed to give 5/7 skewed ladder. Here ‘ i ’ is the index of the unit cell and the numerals 1, 2, ... are numbering of the spins within the unit cell. There are 2 spins per unit cell in the zigzag ladder while there are 8 spins per unit cell in the 5/7 ladder. The sites on the top leg are even numbered and on the bottom leg are odd numbered.

weak and correlations along the leg remain short ranged. Whereas, for $J_1 > 1.5$, gs is magnetic and each unit cell contributes spin 1 to the gs spin S_G , and spin densities are distributed over the whole unit cell, with spin density at sites 3 and 7 being large. For $4.8 < J_1 < 5.9$ the system is nonmagnetic but for $J_1 > 5.9$ gs of the system is magnetic with each unit cell contributing spin 2 to S_G and rung dimers are strong reminiscent of the PSSS state and site spin densities are prominent.

This paper is divided into four sections. In section II we discuss the model Hamiltonian and the numerical methods. The results are presented and discussed in section III in three subsections. Section IV provides a summary of results and conclusions.

II. MODEL AND METHOD

The site numbering used in this paper for the 5/7 skewed ladder is shown in Fig. 1(b). All nonzero exchange interactions between spins are antiferromagnetic. The sites are numbered such that odd numbered sites are on the bottom leg and even numbered sites are on the top leg. Thus the rung bonds are the nearest neighbor exchanges J_1 and the bonds on the legs are the next nearest neighbor exchanges J_2 . The exchange J_2 is set to 1 and it defines the energy scale. The model Hamiltonian

of 5/7 skewed ladder can be written as

$$H_{5/7} = J_1 \sum_i \left(\vec{S}_{i,1} \cdot \vec{S}_{i,2} + \vec{S}_{i,4} \cdot \vec{S}_{i,5} \right) + J_2 \sum_i \left(\vec{S}_{i,7} \cdot \vec{S}_{i+1,1} + \vec{S}_{i,8} \cdot \vec{S}_{i+1,2} + \sum_{k=1}^6 \vec{S}_{i,k} \cdot \vec{S}_{i,k+2} \right). \quad (1)$$

where i labels the unit cell and k the spins within the unit cell (Fig. 1). The first term denotes the rung exchange terms, the second term denotes the exchange interactions along the legs.

We use exact diagonalization (ED) technique for finite ladders with up to 16 spins and impose periodic boundary condition (PBC). There are mirror planes perpendicular to the ladder for example, the plane perpendicular to the ladder and passing through site 3 and the perpendicular bisector of sites 2 and 4 as well as one passing through site 7 and the perpendicular bisector of sites 6 and 8, again perpendicular to the ladder. An extra rung is needed when open boundary condition is used. For larger system sizes we use the density matrix renormalization group (DMRG) method^{29–32} to handle the large degrees of freedom in the many body Hamiltonian. We retain up to 500 block states ($m = 500$) which are the eigenvectors of the block density matrix with dominant eigenvalues. The chosen value of ‘ m ’ keeps the truncation error to less than $\sim 10^{-10}$. We also carry out 6-10 finite sweeps for improved convergence. The details of building the 5/7 ladder for the DMRG method is the same as in Ref. 43. The largest system size studied is a system with 130 sites or 16 unit cells with OBC. The DMRG calculations are carried out for different S^z values of ladders. The gs spin is $S_G = n$, for n that satisfies $\Gamma_n = 0$ and $\Gamma_{n+1} > 0$, where Γ_n is given by

$$\Gamma_n = E_0(S^z = n) - E_0(S^z = 0). \quad (2)$$

with E_0 being the lowest energy state in the chosen S^z sector. The correlation function and bond orders are computed in the gs, with $S^z = S$.

III. RESULTS AND DISCUSSIONS

In the gs, the spin-1 5/7 skewed ladder, like the spin-1/2 system, also shows many exotic phases like the bond-order wave (BOW) phase, chiral order phase and nonmagnetic to magnetic phase transition on tuning the value of J_1 . However, there are significant differences from the spin-1/2 system. To analyze the magnetic transitions in the quantum phase diagram various quantities are analyzed as function of J_1/J_2 which is the only variable model parameter in this system and J_2 is set to 1. Besides the spin gaps Γ_n , we have computed correlation function $C(r) = \langle \vec{S}_l \cdot \vec{S}_{l+r} \rangle$ to study the behavior of the

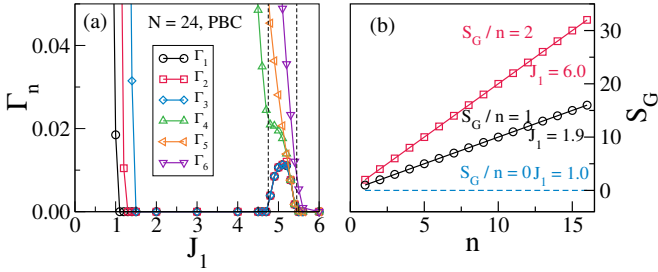


FIG. 2. (a) The lowest excitation gaps Γ_n for different $n = S_G$ manifolds are shown as function of J_1 . For $J_1 < 1.0$, Γ_1 is nonzero, whereas for $1.5 < J_1 < 4.7$, the Γ_n is zero for $n \leq S$ where S is the total spin of the gs. The system exhibits re-entrant antiferromagnetic phase for $4.8 < J_1 < 5.9$ and where Γ_1 is nonzero. For $1.5 < J_1 < 4.7$ $S_G \sim n$ and for $J_1 > 5.9$ $S_G \sim 2n$.

spins in the system. The bond order between bonded neighbors $\langle \vec{S}_l \cdot \vec{S}_{l'} \rangle$ where sites l and l' are bonded neighbors, and spin density $\langle S_l^z \rangle$ within a unit cell are also calculated and compared with results for a 1D spin-1 chain where appropriate.

A. Magnetic ground state

The spin in the gs, S_G , of the skewed 5/7 ladder systems is obtained from the magnetic gaps Γ_n defined in Eq. 2. In Fig. 2(a), we plot the gaps Γ_n for different values of ' n ', as a function of J_1 for a system with 24 spins corresponding to 3 unit cells under OBC. The plot shows that there are four distinct regions: in region I with $0 < J_1 < 1.1$, the gs is a singlet and nonmagnetic, in region II, $1.1 < J_1 < 4.7$, S_G is less than or equal to the number of unit cells in the systems, consequently each unit cell contributes at most spin 1 to S_G and for $1.5 < J_1 < 4.75$, the spin S_G saturates to number of unit cells. In region III, $4.8 < J_1 < 5.9$, the gs becomes nonmagnetic. This re-entrant phase was also observed in the spin-1/2, 5/7 skewed ladder, albeit for much lower J_1 values. In region IV, with $J_1 \geq 6$, S_G corresponds to twice the number of unit cells. In Fig. 2(b), we show the dependence of S_G on system size for two different values of J_1 .

B. Spin correlations

To understand the spin structure in different regions of the parameter space, we have studied the spin-spin correlations of the total spin $C(r) = \langle \vec{S}_k \cdot \vec{S}_{k+r} \rangle$, where k is the reference site of spins in the middle of the system. The z -component of the spin correlations, $C^{zz}(r) = \langle S_k^z S_{k+r}^z \rangle - \langle S_k^z \rangle \langle S_{k+r}^z \rangle$, shows behavior similar to total spin correlation. The total spin correlations are shown for a system of 98 spins, which corresponds to 12 unit cells for open boundary condition. These are calculated

in the gs with $S^z = S_G$. There are three different spin correlations that we have computed. They correspond to the correlation between spins on the lower leg $C_1(49, 49+2r)$, $C_2(50, 50+2r)$ between spins on the upper leg and $C_3(51, 51+4r)$ between “free” spins which reside on the lower leg. The reference site for the correlations are from the middle unit cell which for C_1 is site 49, C_2 is site 50 and for C_3 is site 51. For convenience, we classify the spins on the lower leg as of two types, type 1 “bound” spins which are bound to three nearest neighbor spins and type 2 as “free” spins, which are the middle sites in the five and seven membered rings.

In Fig. 3, we show the spin correlations in the four different regions of the parameter space. The correlations $C_1(r)$ shown in Fig. 3(a) correspond to spins in the lower leg. The correlations are given from site 49 which is in the middle of the system. We note that for $J_1 = 1.0$, the system has a singlet gs. The correlations fall off rapidly and the correlation length ξ is ~ 2.2 sites of the specified kind. In the spin-1 antiferromagnetic chain the correlation length is longer by almost a factor of three and is approximately six sites. The shorter correlation length can perhaps be attributed to the frustration in exchange interactions in the rings. For $J_1 = 2.0$ and 6.0 , the system is in a magnetic state, $C_1(r)$ decays very slowly and is antiferromagnetic in nature. In the re-entrant phase the system goes to a nonmagnetic state and the spin correlations between the spins on the lower leg has long wavelength spin oscillations whose amplitude shows an exponential decay and corresponds to a non-collinear spin arrangement. From the spin correlations, it appears that the magnetic unit cell is tripled in this region. In Fig. 3(b), $C_2(r)$ in the upper leg are shown for the four phases, with the reference spin being the 50th spin in the system. $C_2(r)$ for both $J_1 = 1$ and 2 are antiferromagnetic and exponentially decaying with correlation length, $\xi \approx 3$. For $J_1 = 5$ and 6 $C_2(r)$ are vanishingly small, the magnitude is less than ≈ 0.05 even for nearest neighbor pair, and show long wave length behaviour. The small correlation in upper leg at high J_1 is due to the strong dimer formation along the rungs and between $(i, 6)$ and $(i, 8)$ sites. The correlations between “free” spins $C_3(r)$ shows a rapid decay in the nonmagnetic state at $J_1 = 1$, while those for $J_1 = 2$ and $J_1 = 6$, the correlations are ferromagnetic. For the $J_1 = 6$, the spins at these sites have almost completely aligned ferromagnetically, while for $J_1 = 2$, the alignment is partially ferromagnetic. This reflects in the net spin of the gs which is $2n$ for the $J_1 = 6$ case and n for the $J_1 = 2$ case. In the re-entrant phase, the free spins in each unit cell are aligned ferromagnetically while the alignment of these spins across unit cells is antiferromagnetic, with large periodicity.

In summary, all the spin correlations are always antiferromagnetic, in the nonmagnetic gs for J_1 in regime I, and the correlation lengths are much shorter than the Haldane chain. For J_1 values in regime-II where $S_G \sim n$, the correlations in the lower leg are antiferromagnetic and very long ranged while those in the upper leg are an-

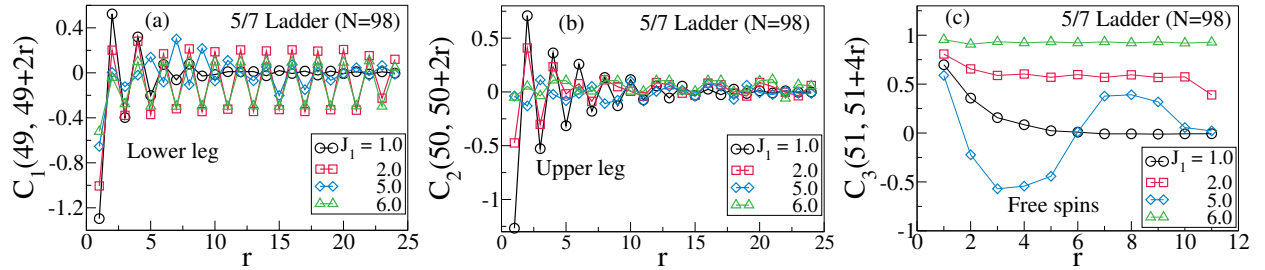


FIG. 3. The spin-spin correlations between (a) spins in the lower leg, (b) spins in the upper leg and (c) free spins at sites 3, 7, 11, etc. for a 5/7 ladder with $N = 98$ spins with OBC. Four J_1 values are chosen to represent different regions of the phase diagram. $J_1 = 1.0$ for non-magnetic phase, $J_1 = 2.0$ for $S_G = n$ phase, $J_1 = 5.0$ for the re-entrant phase and $J_1 = 6.0$ for $S_G = 2n$ phase.

tiferromagnetic and fall off rapidly. The “free” spin correlations are ferromagnetic with an amplitude of about 0.6 and show very slow decay. When the J_1 value is in the re-entrant regime III, the lower leg spin correlations show formation of wave packets over approximately three unit cells. The “free” spin correlations show a long wavelength oscillatory behavior with a three unit cell wavelength, which corresponds to a long period Néel arrangement of “free” spins. In regime IV, the “bound” spins on the lower leg are antiferromagnetically aligned and the correlations fall off very slowly with distance. The correlations between spins on the upper leg show weak long period Néel structure. The “free” spins are aligned ferromagnetically with very long correlation length.

C. Spin densities and bond order

The correlation lengths in the system are short, often less than distance to a third equivalent nearest neighbors. Hence, we can get qualitatively correct behavior of the system in the thermodynamic limit from high accuracy DMRG studies on a system with three unit cells. We have carried out studies on a 24 site spin-1 system, with cyclic boundary conditions, which corresponds to three unit cells. The DMRG accuracy is established by comparing the DMRG bond orders and spin densities for a two unit cell calculations, with exact diagonalization calculations. We have computed the spin densities in the gs for $S^z = S_G$ and the bond orders of all the nearest neighbor bonds. The system has reflection symmetry and hence there are five unique bonds and five unique sites. The spin densities are computed as the expectation value of $\langle \psi_{gs} | S_i^z | \psi_{gs} \rangle$. They are uniformly zero in the singlet gs. The bond orders are computed as $b_{i,j} = \langle \psi_{gs} | S_i \cdot S_j | \psi_{gs} \rangle$, where i and j are nearest neighbor bonds. When the gs of the system is a singlet (region I), from the bond orders (Fig. 4) we can describe the system as weakly coupled spin-1 HAF chains. The upper leg is a bond order wave (BOW) with a periodicity of four bonds while the lower is a BOW with a periodicity of two bonds. The rung bonds are weak and the leg bond orders vary between -1.370 and 1.285 . For comparison,

in the spin-1 HAF, all the bond orders are uniform and have a value of -1.43 . In region II, where $S_G = n$, the upper leg bond between the sites in the pentagon become weak, the rung bonds become strong and the bonds in the lower leg also become slightly weak. Besides, the bond on the upper leg between the sites which entirely belongs to the seven membered ring also becomes strong. The rung bonds become much stronger while the ladder bonds become weaker. The amplitude of the BOW on both the legs increase, but on the lower leg, the phase of the wave is shifted by π . The spin densities at the “free” spin sites are nearly equal and there is a net negative spin density on the rung bonds with the spin density of the sites on the lower leg being large negative. The “bonded” spin sites on the seven membered ring on the upper leg acquire small negative spin densities. In region IV, where the $S_G = 2n$, the rung bonds and the bond in the upper leg of the seven membered ring almost form singlets, with a bond order close to -2 . All other bonds are very weak. The spin density of the sites in the seven membered ring which form the singlet are very nearly zero, while the rung bonds are qualitatively different with large negative (on the lower leg) and positive (on the upper leg) spin densities. The “free” spins are almost completely polarized and have spin densities which are very nearly unity. We show the correlations between “free” spins at Fig. 3(c). In region II the $(3, 7)$ spin correlation is close to the $S = 2$ value of 1, and reaches the value of 1 in region IV. In region I, the value is positive, indicating substantial ferromagnetic alignment of the “free” spins within the unit cell. In the re-entrant region III, this has the lowest value and indeed the spin correlations for the next-nearest and next to next-nearest neighbor are negative, indicating antiferromagnetic alignment of these spins with the reference spin.

The spin-1 skewed ladder is very different from a spin-1 chain as we can see from the bond orders. The gs of the spin-1 chain can be represented as an AKLT state. However, the bond order pattern reveals that only in region IV, the gs can be approximated by three singlets and a spin-2 state involving free spins, and in none of the regions we can approximate the gs by an AKLT state, just as in regular ladders.

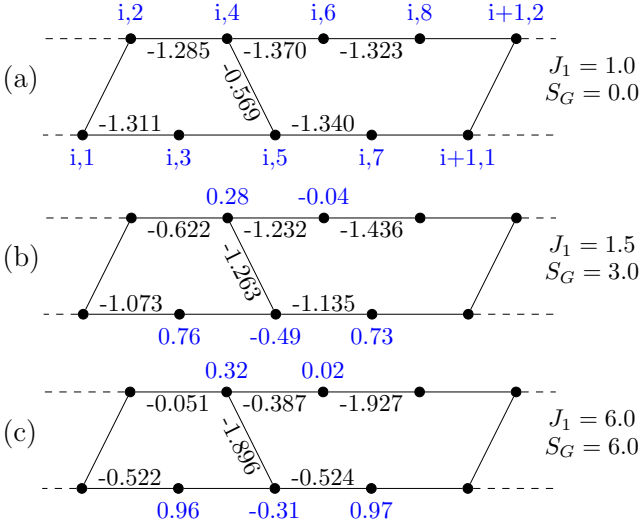


FIG. 4. Bond order for 5/7 skewed ladder with $N = 24$ spins considering a periodic boundary condition in three different region: (a) nonmagnetic at $J_1 = 1.0$, (b) $S_G = n$ at $J_1 = 1.5$ and (c) $S_G = 2n$ at $J_1 = 6.0$. The numbers above the bonds is the spin-spin correlation between the spins shared by the bond and the numbers below the bonds is the longitudinal spin-spin correlation between the same. The site index is given for (a) and the spin density is given for the case (b) and (c) in blue.

D. Vector chiral phase and the BOW phase

Broken symmetry states give rise to different quantum phases whose properties depend on the type of symmetry that is broken in the system. In general broken spatial inversion/reflection symmetry gives rise to bond order wave (BOW) phase, whereas broken spin inversion symmetry gives rise to spin density wave (SDW). If both the spatial and spin inversion symmetries in the system are broken then the vector chiral phase arises and it leads to spontaneous spin current in the system. For these symmetries to break simultaneously, the lowest energy states in the two subspaces that the symmetry element divides the appropriate Hilbert space should be degenerate. In this case, any linear combination of the two low-lying states in the two subspaces which are even (odd) under both reflection and spin inversion will be degenerate resulting in symmetry breaking. The symmetry group of the 5/7 skewed ladder system consists of four elements; E , P , σ and σP and all these elements commute with each other leading to an Abelian group. The four irreducible representation correspond to A^+ , A^- , B^+ , B^- . A (B) corresponds to even (odd) under σ while $'+'$ $'-'$ corresponds to even (odd) under P . A BOW transition requires a degeneracy between the lowest states in A^+ and B^+ or A^- and B^- subspaces. Similarly an SDW transition requires a degeneracy of the lowest energy states in A^+ and A^- or B^+ and B^- subspaces. For a vector chiral transition, the lowest energy states in A^+ and B^- or A^- and B^+

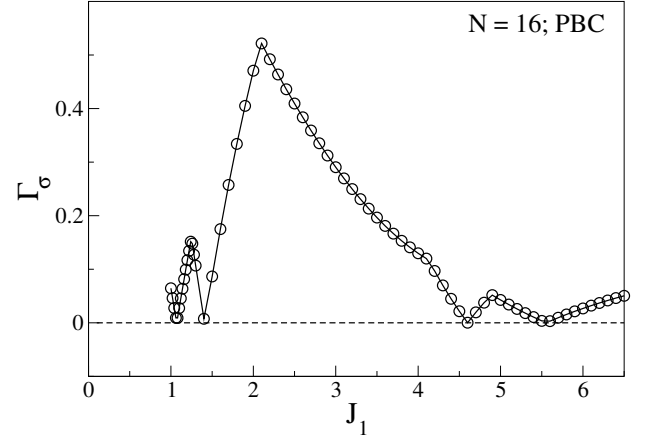


FIG. 5. The energy gap Γ_σ (see Eq. 3) between two lowest energy levels belonging to different reflection symmetry subspaces. Γ_σ vanishes at $J_1 = 1.07$, 1.408 , 4.601 and 5.55 indicating degeneracies at these J_1 values.

subspaces must be degenerate.

The spin inversion symmetry, P divides the $S^z = 0$ subspace into even and odd total spin (S) sectors, and the lowest energy states of the odd and even subspaces under P should be degenerate to break the spin inversion symmetry. To determine the degeneracy under spin inversion symmetry, instead of exploiting the fact that ' P ' divides the Hilbert space with $S^z = 0$ into even and odd total spin subspaces, we use the following argument. Whenever there is a degeneracy of the lowest energy states with odd and even total spins, then the spin inversion symmetry is broken. We recognize the degeneracy of the gs when two states in the $S^z = 0$ sector are degenerate. In this case, we compute the energies of the lowest states in the higher S^z sectors. The spin of the degenerate spin states are determined by following the degeneracies of the states in these sectors. Thus, from table I, we find that for $J_1 = 1.07$, the two degenerate gs are with spins $S = 0$ and 1 . Similarly, for $J_1 = 1.408$, states with $S = 1$ and $S = 2$, for $J_1 = 4.601$, states with $S = 2$ and $S = 3$, for $J_1 = 5.55$, $S = 3$ and $S = 4$ form degenerate ground states. We also calculate the energy gap Γ_σ as the modulus of the difference in energy between the lowest energy states in the A and B subspaces defined as

$$\Gamma_\sigma = |E_0(\sigma = -1) - E_0(\sigma = +1)|, \quad (3)$$

where $E_0(\sigma = +1)$ and $E_0(\sigma = -1)$ are the lowest energies in the even and odd subspaces under σ . We show in Fig. 5 that Γ_σ goes to zero for these values of J_1 and hence we expect a vector chiral transition and nonzero spin currents. Usually, in all known systems this happens either due to anisotropy or due to an external magnetic field. The consequence of breaking these symmetries leads to a spin current in the rings. The skewed ladder system is unusual as the spin current exists in the absence of both anisotropy and external magnetic field. The spin current

TABLE I. Two lowest energy levels from different S^z sectors at specified J_1 values (see Fig. 5).

J_1	$E(S^z = 0)$	$E(S^z = 1)$	$E(S^z = 2)$	$E(S^z = 3)$	$E(S^z = 4)$
1.07	-23.8471	-23.8470			
	-23.8470				
1.408	-25.0575	-25.0575	-25.0574		
	-25.0574	-25.0574			
4.601	-44.7871	-44.7871	-44.7871	-44.7871	
	-44.7871	-44.7871	-44.7871		
5.55	-51.7948	-51.7948	-51.7948	-51.7948	-51.7946
	-51.7946	-51.7946	-51.7946	-51.7946	

can be calculated as the matrix element of the operator $\kappa_{j,k}$ given by

$$\kappa_z(j, k) = \langle \psi_G(-) | \vec{S}_j \times \vec{S}_k | \psi_G(+) \rangle = (i/2) \langle \psi_G(-) | S_j^+ S_k^- - S_j^- S_k^+ | \psi_G(+) \rangle, \quad (4)$$

where the function $| \psi_G(+) \rangle$ ($| \psi_G(-) \rangle$) is the gs in the even (odd) subspace for reflection and even(odd) subspace for spin inversion. In Fig. 6, we show the spin currents for $J_1 = 1.408$ and 5.550 for different degenerate S^z values. We find that the spin currents are large for $J_1 = 1.408$ compared to $J_1 = 5.550$. At $J_1 = 1.408$, the spin current is larger in the five membered ring compared to that in the seven membered ring. Also, the direction of spin currents are opposite in the two rings. The spin currents are also not uniform for all the bonds. The ladder bonds have smaller currents than the leg bonds and in the five membered ring, the upper leg has larger currents than the lower ring, while it is the opposite in the seven membered ring. The spin current in the five membered ring almost vanishes at $J_1 = 5.550$ while it is much weaker in the seven membered ring. The spin currents of the rung bonds are very small and the spin current on the leg bonds in the seven membered ring become uniform. There is also weak dependence of the spin current current on the S^z value of the state for which it is calculated.

IV. SUMMARY AND CONCLUSION

In this paper we study quantum phases of spin-1 Heisenberg antiferromagnetic model on a 5/7 ladder shown in Fig. 1(b). This system goes from a non-magnetic state to partially magnetized state for $J_1 > 1.1$, and for $J_1 > 1.5$ magnetization per unit cell is $\langle m \rangle = 1$. The gs again goes to a non-magnetic state for $4.8 < J_1 < 5.9$, and spins have non-collinear arrangement in this phase. For large $J_1 > 5.9$ the gs goes to magnetic state with $\langle m \rangle = 2$.

The correlation length in the 5/7 ladder decreases monotonically with J_1 and for $J_1 = 1$ the correlation length $\xi \sim 3$ lattice units in the singlet gs. The bond-order along the leg increases monotonically with J_1 , and in large J_1 limit the gs is product of rung dimers and free

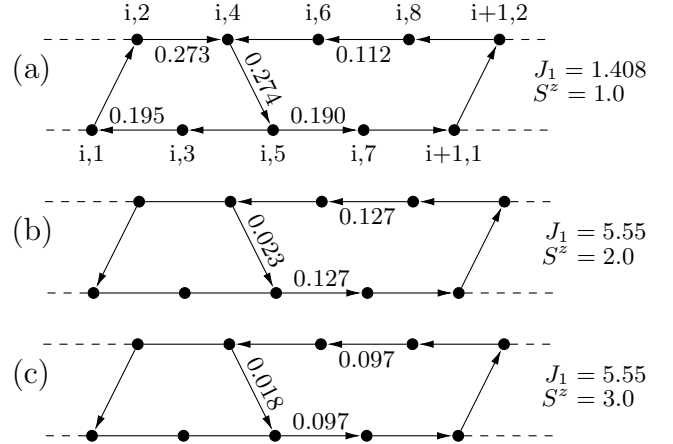


FIG. 6. Spin currents $\kappa_z(j, k)$ of a 5/7 skewed ladder of $N = 16$ spins (see Eq. 4) for (a) $J_1 = 1.408$ in the $S^z = 1$ sector, (b) $J_1 = 5.55$ in the $S^z = 2$ sector, (c) $J_1 = 5.55$ in the $S^z = 3$ sector. Arrows indicate the direction of the current and the magnitude of the currents are given adjacent to the arrows. No arrowhead for a bond means the spin current is zero along that bond.

spin at 3 and 7 site of an unit cell. Uniform VBS state of spin-1 chain disappears even for small value of J_1 as spin-1/2 at the edges of the ladder get pinned by rung interaction and form singlet pairs. However, dimers are formed both along the rung and leg even for any non-zero value of J_1 . In large J_1 limit the spins at sites $8n - 2$ and $8n$ forms a strong singlet dimer which is comparable to a spin-1 singlet dimer with bond order ~ -2.0 .

For $J_1 < 1.1$, Γ_σ vanishes and reflection symmetry is broken leading to dimer order in the system. For larger J_1 values the gs is in ferrimagnetic state and for some J_1 values the lowest energy states in the even-even and odd-odd subspace under reflection and spin inversion become degenerate. This leads to both inversion and spin parity symmetry being broken, therefore, the gs is in vector chiral phase and there is spontaneous spin current in the ladder system. This is unique as it can have both finite magnetization and spin current in the absence of external magnetic field. In this system maximum gs magnetization per unit cell, $\langle m \rangle = 2$, while, for a spin-1/2

system $\langle m \rangle = 1^{43,45}$. In the spin-1/2 system magnetic moments are localized mostly on $(4n - 1)$ sites of the system and other sites have vanishingly small spin density^{43,45}. However, in spin-1 system while magnetization contribution comes mostly from sites $(4n - 1)$, there is antiferromagnetically aligned spin density in the lower leg and ferromagnetically aligned spins in upper leg due to strong singlet dimer formation along the rung. The isolated singlet spin-1 dimer between sites $8n - 2$ and $8n$ in this extended system is unique.

In conclusion, HAF spin-1 system on a skewed 5/7 ladder is unique with different ferrimagnetic gs, and this system exhibits a plethora of exotic phases in the gs on tuning J_1 . The spin arrangements of spin-1 system is vastly different from that on spin-1/2 on this lattice. This is a unique ladder system where singlet spin-1 dimer and

bond order wave can co-exist. The topological phase of spin-1 chain vanishes for any finite value of J_1 . The HAF 5/7 ladder system can be mapped on to a spin-1 chain with antiferromagnetic nearest and next nearest neighbor interaction J_1 and J_2 with periodically missing J_1 bonds. This system may be realized in molecular magnets based on transition metal compounds.

ACKNOWLEDGMENTS

MK thanks Department of Science and Technology (DST), India for Ramanujan fellowship. SR thanks Indian National Science Academy and DST-SERB for supporting this work.

SD and DD contributed equally to this work.

* sambunath.das46@gmail.com
 † dayasindhu.dey@gmail.com
 ‡ manoranjan.kumar@bose.res.in
 § ramaresh@iisc.ac.in

¹ C. K. Majumdar and D. K. Ghosh, *J. Math. Phys.* **10**, 1388 (1969); *J. Math. Phys.* **10**, 1399 (1969).
² T. Hamada, J.-i. Kane, S.-i. Nakagawa, and Y. Natsume, *J. Phys. Soc. Jpn.* **57**, 1891 (1988).
³ A. V. Chubukov, *Phys. Rev. B* **44**, 4693 (1991).
⁴ R. Chitra, S. Pati, H. R. Krishnamurthy, D. Sen, and S. Ramasesha, *Phys. Rev. B* **52**, 6581 (1995).
⁵ S. R. White and I. Affleck, *Phys. Rev. B* **54**, 9862 (1996).
⁶ C. Itoi and S. Qin, *Phys. Rev. B* **63**, 224423 (2001).
⁷ S. Mahdavifar, *J. Phys.: Condens. Matter* **20**, 335230 (2008).
⁸ J. Sirker, *Phys. Rev. B* **81**, 014419 (2010).
⁹ M. Kumar, A. Parvej, and Z. G. Soos, *J. Phys.: Condens. Matter* **27**, 316001 (2015).
¹⁰ Z. G. Soos, A. Parvej, and M. Kumar, *J. Phys.: Condens. Matter* **28**, 175603 (2016).
¹¹ M. Kumar, S. Ramasesha, and Z. G. Soos, *Phys. Rev. B* **81**, 054413 (2010).
¹² M. Kumar and Z. G. Soos, *Phys. Rev. B* **85**, 144415 (2012).
¹³ T. Vekua, A. Honecker, H.-J. Mikeska, and F. Heidrich-Meisner, *Phys. Rev. B* **76**, 174420 (2007).
¹⁴ T. Hikihara, L. Kecke, T. Momoi, and A. Furusaki, *Phys. Rev. B* **78**, 144404 (2008).
¹⁵ J. Sudan, A. Lüscher, and A. M. Läuchli, *Phys. Rev. B* **80**, 140402(R) (2009).
¹⁶ D. V. Dmitriev and V. Y. Krivnov, *Phys. Rev. B* **77**, 024401 (2008).
¹⁷ F. Heidrich-Meisner, A. Honecker, and T. Vekua, *Phys. Rev. B* **74**, 020403(R) (2006).
¹⁸ F. Heidrich-Meisner, I. A. Sergienko, A. E. Feiguin, and E. R. Dagotto, *Phys. Rev. B* **75**, 064413 (2007).
¹⁹ F. Heidrich-Meisner, I. P. McCulloch, and A. K. Kolezhuk, *Phys. Rev. B* **80**, 144417 (2009).
²⁰ A. Parvej and M. Kumar, *Phys. Rev. B* **96**, 054413 (2017).
²¹ L. Kecke, T. Momoi, and A. Furusaki, *Phys. Rev. B* **76**, 060407(R) (2007).
²² F. D. M. Haldane, *Phys. Lett.* **93A**, 464 (1983); *Phys. Rev. Lett.* **50**, 1153 (1983).
²³ I. Affleck, T. Kennedy, E. H. Lieb, and H. Tasaki, *Phys. Rev. Lett.* **59**, 799 (1987).
²⁴ I. Affleck, T. Kennedy, E. H. Lieb, and H. Tasaki, *Communications in Mathematical Physics* **115**, 477 (1988).
²⁵ U. Schollwöck, O. Golinelli, and T. Jolicoeur, *Phys. Rev. B* **54**, 4038 (1996).
²⁶ S. Östlund and S. Rommer, *Phys. Rev. Lett.* **75**, 3537 (1995).
²⁷ F. Verstraete, V. Murg, and J. Cirac, *Adv. Phys.* **57**, 143 (2008).
²⁸ U. Schollwöck, *Ann. Phys.* **326**, 96 (2011).
²⁹ S. R. White, *Phys. Rev. Lett.* **69**, 2863 (1992).
³⁰ S. R. White, *Phys. Rev. B* **48**, 10345 (1993).
³¹ U. Schollwöck, *Rev. Mod. Phys.* **77**, 259 (2005).
³² K. A. Hallberg, *Advances in Physics* **55**, 477 (2006).
³³ R. Orús, *Ann. Phys.* **349**, 117 (2014).
³⁴ F. Verstraete and J. I. Cirac, *Phys. Rev. A* **70**, 060302(R) (2004).
³⁵ T.-C. Wei, I. Affleck, and R. Raussendorf, *Phys. Rev. Lett.* **106**, 070501 (2011).
³⁶ M. Lemm, A. W. Sandvik, and L. Wang, *Phys. Rev. Lett.* **124**, 177204 (2020).
³⁷ N. Pomata and T.-C. Wei, *Phys. Rev. Lett.* **124**, 177203 (2020).
³⁸ D. Dey, M. Kumar, and Z. G. Soos, *Phys. Rev. B* **94**, 144417 (2016).
³⁹ S. R. White and D. A. Huse, *Phys. Rev. B* **48**, 3844 (1993).
⁴⁰ S. Todo, M. Matsumoto, C. Yasuda, and H. Takayama, *Phys. Rev. B* **64**, 224412 (2001).
⁴¹ T. Hikihara, M. Kaburagi, and H. Kawamura, *Prog. Theor. Phys., Suppl.* **145**, 58 (2002).
⁴² N. Chepiga, I. Affleck, and F. Mila, *Phys. Rev. B* **93**, 241108(R) (2016).
⁴³ G. Giri, D. Dey, M. Kumar, S. Ramasesha, and Z. G. Soos, *Phys. Rev. B* **95**, 224408 (2017).
⁴⁴ S. Thomas, S. Ramasesha, K. Hallberg, and D. Garcia, *Phys. Rev. B* **86**, 180403(R) (2012).
⁴⁵ D. Dey, S. Das, M. Kumar, and S. Ramasesha, *Phys. Rev. B* **101**, 195110 (2020).